DOI: 10.1002/asia.201300303

Cell-Based Proteome Profiling Using an Affinity-Based Probe (A*f*BP) Derived from 3-Deazaneplanocin A (DzNep)

Eric K. W. Tam,[a] Zhengqiu Li,[b] Yi Ling Goh,[a] Xiamin Cheng,[b] Sze Yue Wong,[a] Sridhar Santhanakrishnan,[a] Christina L. L. Chai,*[a, c] and Shao Q. Yao*[b]

Abstract: 3-Deazaneplanocin A (DzNep), a global histone methylation inhibitor, has attracted significant interest in epigenetic research in recent years. The molecular mechanism of action and the cellular off-targets of DzNep, however, are still not well-understood. Our aim was to develop novel DzNep-derived small-molecule probes suitable to be used in live mammalian cells for identification of potential cellular targets of DzNep under physiologically relevant settings. In the current study, we have successfully designed, synthesized, and tested one such probe, called DZ-1. DZ-1 is a 'clickable' affinity-based probe (A*f*BP) derived from DzNep with minimal structural modifications. The probe was found to be highly cell-permeable, and possessed similar anti-apoptotic activities as DzNep in MCF-7 mammalian cells. Two additional control probes were made as negative labeling/pull-down probes in order to minimize false identification of background proteins due to unavoidable, intrinsic nonspecific photo-crosslinking reactions. All three probes were subsequently used for in-situ proteome profiling in live mammalian cells, followed by large-scale pull-down/LC-MS/MS analysis for identification of potential cellular protein targets that might interact with DzNep in native cellular environments. Our LC-MS/MS results revealed some highly enriched proteins that had not been reported as potential DzNep targets. These proteins might constitute unknown cellular off-targets of DzNep. Though further validation experiments are needed in order to unequivocally confirm these off-targets, our findings shed new light on the future use of DzNep as a validated chemical probe for epigenetic research and as a potential drug candidate for cancer therapy.

Keywords: affinity-based probes · click chemistry · epigenetics · inhibitors · proteomics

Introduction

Post-translational modification of histones is an essential event for the regulation of chromatin structure and gene expression in eukaryotes. 3-Deazaneplanocin A (DzNep, Figure 1) is a carbocyclic analog of adenosine that was originally developed as a potent inhibitor of *S*-adenosylhomocysteine hydrolase (SAHH) for potential therapeutic applications.[1] In recent years, there has been renewed interest in the application of DzNep in epigenetic research, primarily due to the discovery that DzNep could modulate histone methylation by disrupting the activity of histone-lysine *N*-methyltransferase EZH2.[2] The latter is a catalytic subunit of the polycomb repressive complex 2 (PRC2) that functions to silence tumor suppressor genes by the addition of three methyl groups to lysine 27 of histone 3, a modification leading to chromatin condensation.[3] EZH2 is also known to associate with numerous cellular proteins, such as the embryonic ectoderm development protein, the VAV1 oncoprotein, and the X-linked nuclear protein (XNP).[4] It may also play a role in the hematopoietic and central nervous systems. EZH2 overexpression has been shown to have implications in tumorigenesis and to correlate with poor prognosis in several tumor types.[5] EZH2 inhibition by DzNep has been documented in cultured cancer cell types, including primary and acute myeloid leukemia (AML) cells.[6,7] For example, human AML cells treated with DzNep were found to have elevated expression levels of several cell-cycle regulators including p21, p27, and FBXO32, before undergoing cell cycle arrest and apoptosis.[6] These findings have led to the pursuit of using DzNep and similar compounds as potential therapeutic agents in the treatment of cancer.[7] Notwithstanding the intensive efforts on DzNep in epigenetic research, existing biochemical and cellular data on DzNep and its poten-

[a] Dr. E. K. W. Tam,[+] Y. L. Goh, S. Y. Wong, Dr. S. Santhanakrishnan, Prof. Dr. C. L. L. Chai
Institute of Chemical and Engineering Sciences
8 Biomedical Grove, Neuros #07-01, 138665 (Singapore)

[b] Dr. Z. Li,[+] X. Cheng, Prof. Dr. S. Q. Yao
Department of Chemistry
National University of Singapore
3 Science Drive 3, 117543 (Singapore)
Fax: (+65) 6779-1691
E-mail: chmyaosq@nus.edu.sg

[c] Prof. Dr. C. L. L. Chai
Department of Pharmacy
National University of Singapore
18 Science Drive 4, 117543 Singapore
E-mail: phacllc@nus.edu.sg

[+] These authors contributed equally to this work.

Supporting information for this article is available on the WWW under http://dx.doi.org/10.1002/asia.201300303.

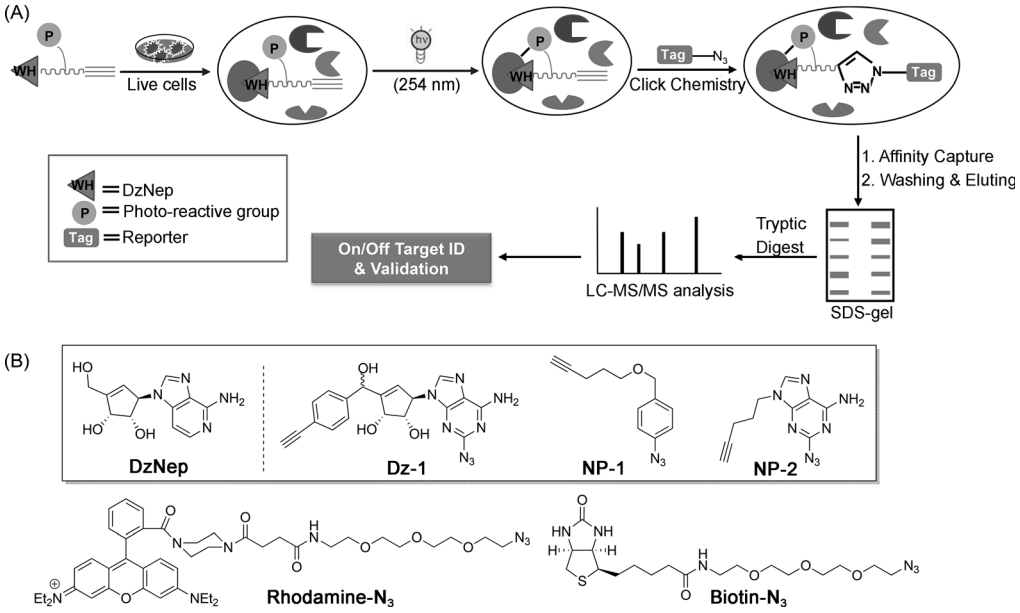

Figure 1. (A) Overall workflow of the cell-based proteome profiling approach followed by large-scale pull-down/LC-MS/MS for identification of potential cellular targets of DzNep using affinity-based probes (A*f*BPs) shown in panel B. (B) Structure of DzNep, the DzNep-derived probe **DZ-1**, and the negative control probes **NP-1** and **NP-2**. The two click reporters, rhodamine-N_3 and biotin-N_3, used in the current study are also shown.

tial biological targets are at best inconclusive.[8] As an adenosyl nucleoside analog, DzNep might be expected to bind to a variety of other cellular proteins that possess intrinsic binding affinity toward AMP/ADP/ATP, *S*-Adenosyl methionine (SAM), NADH/NADPH, and other nucleotide analogs, in addition to its putative targets SAHH and EZH2. Many such proteins are present in mammalian cells, including kinases, methyltransferases, ATPases, oxidoreductases, and others. It is therefore imperative to decipher the precise molecular targets of DzNep and to elucidate its mechanism of action. Strategies capable of large-scale proteome-wide analysis and identification of potential cellular targets of DzNep under physiological settings have, however, not been reported thus far.

Several chemical profiling strategies for large-scale, proteome-wide protein target identification exist, but most of them use affinity beads immobilized with the compound of interest (e.g., the probe) to capture its interacting proteins from cellular lysates.[9,10] In more recent examples, protein–drug interactions were studied under native cellular settings by adding the drug of interest directly to cells and initiate binding to its intended cellular targets. Upon cell lysis, immobilized probes were then added to the cell lysates as "baits". By measuring the amount of a protein captured on beads by quantitative mass spectrometry, with and without drug treatment, this method, when compared to previous methods,[9] is a step forward in the right direction and enables the in-situ profiling of protein–drug interactions indirectly.[10] Nevertheless, the strong reliance on bead-bound probes and/or cellular lysates to capture protein–drug interactions inevitably leads to many ''false positives'' and ''missed targets'' in all these strategies, as genuine protein–drug interactions (defined hereafter as those that occur in living cells under physiologically relevant conditions) are governed by a variety of other factors besides the protein/ligands themselves, including protein compartmentalization and localized protein concentrations. Our long-term research aim has been to develop chemical strategies capable of interrogating protein–drug interactions in native cellular environments (i.e., in live cells, not cell lysates).[11,12] This calls for the design of small-molecule probes that are cell-permeable, minimally disrupt protein–drug interactions, and effectively capture interacting cellular targets in situ (Figure 1 A).[12] Previously, we had successfully carried out several large-scale liquid chromatography–tandem mass spectrometry (LC-MS/MS) experiments on small-molecule drugs (e.g., Orlistat and Dasatinib) by using such design principles.[12a,c] From these studies, we have firmly established that such a cell-based proteome profiling approach is indeed effective in the rapid identification of potential cellular targets of biologicallly relevant small molecules. A key element to the success of this approach is the design of suitable cell-permeable, small-molecule probes that are modified versions of the target compounds but are capable of recapitulating most if not all the genuine protein–interacting events under physiological settings (Figure 1 B). As part of our on-going interest in DzNep and related compounds, we have undertaken the challenge of developing DzNep-derived probes that might be useful for identification of potential cellular targets (both on- and off-targets) of DzNep. Herein, we report the successful design, synthesis, and biological testing of DZ-1 (Figure 1 B&Scheme 1), a 'clickable' affinity-based probe (A*f*BP) derived from DzNep with minimal structural modifications. The probe was found to be highly cell-permeable

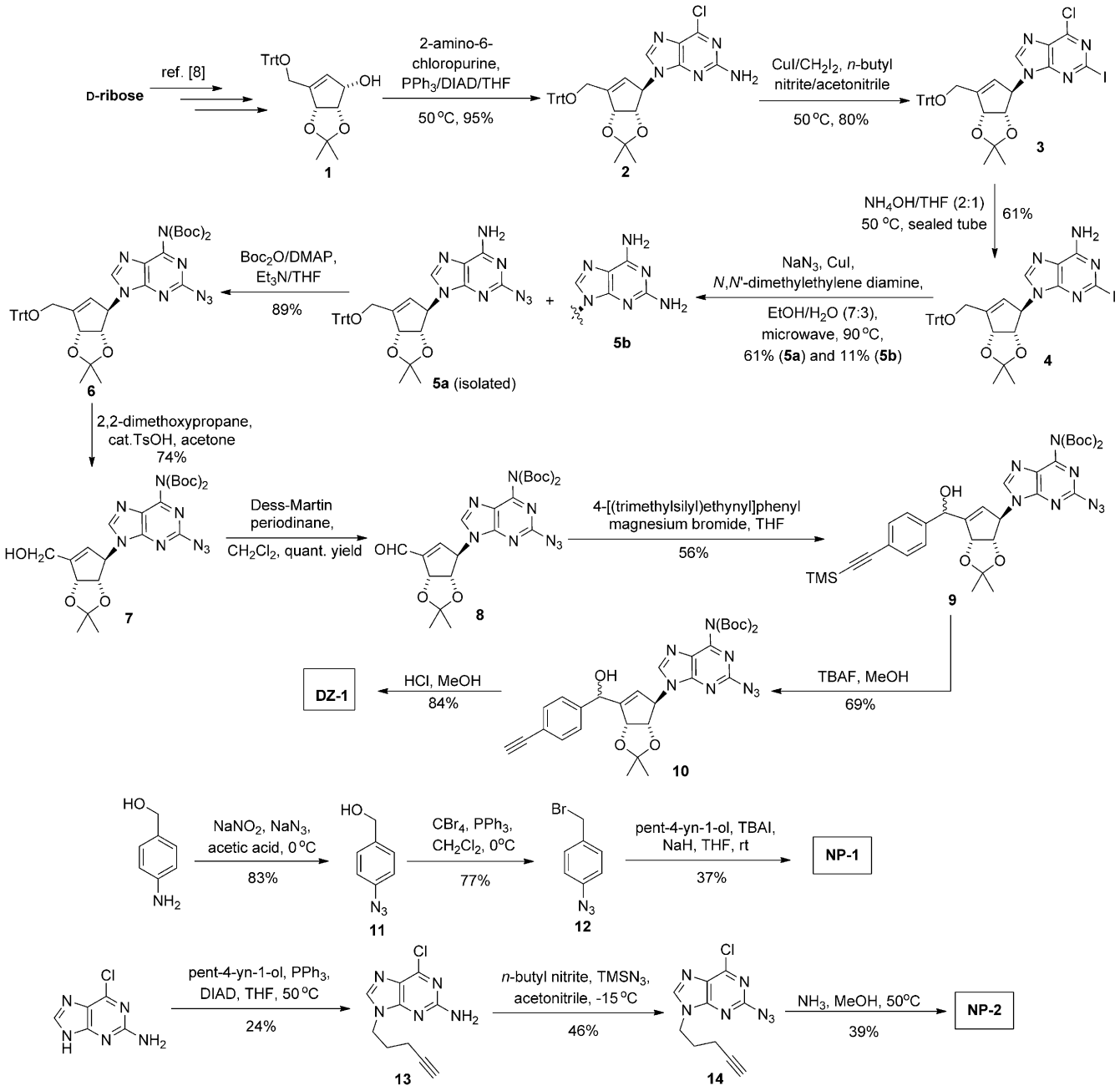

Scheme 1. Synthesis of probes **DZ-1**, **NP-1**, and **NP-2** used in this study. DIAD = diisopropyl azodicarboxylate, DMAP = 4-dimethylaminopyridine, TBAF = tetra-*n*-butylammonium fluoride, TBAI = tetrabutylammonium iodide, $TMSN_3$ = trimethylsilyl azide.

and to possess similar anti-apoptotic activities as DzNep in MCF-7 mammalian cells. We have successfully carried out in-situ proteome profiling of DZ-1 in MCF-7 cells, followed by large-scale pull-down LC-MS/MS analysis for the identification of potential cellular protein targets of DzNep. Our LC-MS/MS results revealed some highly enriched proteins that were previously unknown DzNep targets. These might constitute potential cellular off-targets of DzNep.

Results and Discussion

Overall Workflow of Cell-Based Proteome Profiling

As shown in Figure 1 A, in our cell-based proteome profiling approach, a cell-permeable DzNep-derived probe (e.g., **DZ-1**) bearing a photoreactive group and an alkyne handle was used to convert non-covalent protein–drug interactions into covalent linkage in situ. Upon cell lysis, these protein–probe cross-linked complexes would be subsequently conjugated to an azide-containing reporter tag (e.g., rhodamine-N_3 or

biotin-N_3) by the well-established bioorthogonal click chemistry.[13] Further in-gel fluorescence scanning and/or pull-down (PD)/LC-MS/MS analysis would enable large-scale identification of potential DzNep-binding cellular proteins. This approach could alleviate many of the aforementioned problems encountered in the 'traditional' PD approaches,[9,10] in that it would enable genuine noncovalent protein–probe intereactions to be faithfully captured in situ prior to downstream in-vitro cell lysis, protein enrichment, and LC-MS/MS analysis for target identification.

Design and Synthesis of DZ-1

The probe **DZ-1** contained several critical elements of design needed for a successful cell-based proteome profiling experiment. First, the probe preserved most of the core structure in DzNep, namely the adenine and the cyclopentendiol moieties, thus retaining most if not all of the protein-binding ability and apoptotic activities when compared with wild-type DzNep (see below). Second, a photo-reactive group that allows conversion of non-covalent protein–probe interaction in situ to covalent linkage upon UV irradiation was introduced into the probe, and this was accomplished through an aryl azide installed at the C_2 position of the adenine group, which retained the essential structural features in adenine and, at the same time, delivered an aryl azide that can be converted into a highly reactive nitrene upon UV irradiation (254 nm). Finally, an aryl alkyne moiety was installed at a position remote from the core pharmacophore. Based on known structure–activity relationships of DzNep analogs and their apoptotic activities (data not shown),[1b] this position was not expected to interfere with protein–probe binding. The alkyne would serve as a convenient click reporter moiety for subsequent detection, purification, and isolation of probe-labeled proteins. For the purpose of reducing false-positive hits, which are intrinsic and in most cases unavoidable in protein photo-crosslinking experiments,[14] two negative probes, **NP-1** and **NP-2** (Figure 1B), were designed and used in all subsequent cell-based proteome profiling and PD/LC-MS/MS experiments.

The synthesis of **DZ-1** is summarized in Scheme 1. It commenced from the optically pure *O*-protected cyclopentendiol **1** which was obtained from D-ribose in 8 steps.[15] Mitsunobu coupling between compound **1** and 2-amino-6-chloropurine gave the single adduct **2** in excellent yield (95%). Unfortunately, subsequent direct amine-to-azide conversion on the purine ring of **2** to deliver the corresponding azide **5a** in a single step was unsuccessful when *n*-butyl nitrite in the presence of trimethylsilylazide or sodium azide was used. Thus, a longer sequence was subsequently employed to achieve the desired chemical transformation through the formation of intermediates **3** and **4**. In this synthetic route, the aromatic amine **2** was initially converted into the corresponding iodide **3** by a diazotization–iodination protocol. This was followed by amination at the 4-chloro position of the purine ring to furnish 4-amino-2-iodoadenine (i.e., compound **4**). Next, the iodo group in **4** was converted into an azido functionality under copper-catalyzed microwave conditions, thereby giving rise to **5a** (61% yield). The corresponding amine side-product **5b** was also obtained in 11% yield. The *exo*-amino functionality on the purine ring of **5a** was then protected as the *N*,*N*-diBoc derivative **6**. Subsequent deprotection of the trityl group in **6** was achieved by treatment with *p*-toluene sulfonic acid to yield the cyclopentendiol **7** in 74% yield. Dess–Martin periodinane oxidation of **7** gave the corresponding aldehyde **8** (quantitative yield), which was used in a subsequent Grignard reaction without further purifications. The Grignard reaction between the aldehyde **8** and 4-[(trimethylsilyl)ethynyl]phenyl magnesium bromide delivered compound **9** as an inseparable 10:1 diastereomeric mixture (56% yield). Finally, deprotection of the TMS group on the alkyne with TBAF and treatment with HCl gave the desired target probe **DZ-1** as a mixture of diastereomers (58% yield over two steps).

The synthesis of the two negative probes, **NP-1** and **NP-2**, is summarized in Scheme 1. Probe **NP-1** was prepared in three steps from (4-aminophenyl)methanol. The first step involved the formation of azide **11** by diazotization–azidation of the aromatic amine starting material with sodium nitrite and sodium azide in acetic acid at 0°C (83% yield). The hydroxy group in **11** was then converted into a bromo group to give **12** (77% yield). The subsequent S_N2 reaction between the alkoxide form of **12** and pent-4-yn-1-ol furnished **NP-1** in 37% yield. The other negative probe, **NP-2**, was synthesized in a three-step route. First, a direct coupling reaction between the chloropurine and pent-4-yn-1-ol was successfully carried out under Mitsunobu reaction conditions (with triphenylphosphine and diethyl azodicarboxylate as coupling reagents) to afford **13** in 24% yield. Next, direct amine-to-azide conversion from **13** into **14** in a single step was successful by using *n*-butyl nitrite and trimethylsilyl azide (TMS-N_3) in acetonitrile at −15°C (46% yield). Finally, amination of the chloro moiety on **14** gave the expected product **NP-2** in 39% yield. All probes including their intermediates were fully characterized by NMR spectroscopy and mass spectrometry before being used in subsequent biological and proteomic experiments.

Biological Evaluation of the Probes

We first assessed the cell permeability of the probes. DzNep was used as the positive reference compound. Many small-molecule probes developed thus far have bulky reporter groups such as a fluorophore or biotin directly attached to the compound of interest.[16] This makes downstream protein analysis and isolation straightforward, but the main problem is that the chemical structure of the resulting probe becomes significantly different from that of the original unmodified compound. Consequently, the biological properties, including cell permeability, cellular localization, and protein-binding ability, of such probes might be significantly altered. Our design of **DZ-1** took a "minimalist" approach to minimize structural changes to DzNep, and we thus expected **DZ-1** and DzNep to possess similar cellular properties including

(A)

Compound	$P_{app\ (A-B)}$ (10^{-6}, cm/s)	$P_{app\ (B-A)}$ (10^{-6}, cm/s)	Efflux Ratio	Recovery (%)	
				A-B	B-A
DZ-1	18.57	19.48	1.05	77.40	92.08
NP-1	10.16	11.44	1.13	29.79	38.22
NP-2	32.35	30.82	0.95	96.67	97.00
DZNep	12.29	18.65	1.52	45.00	77.65

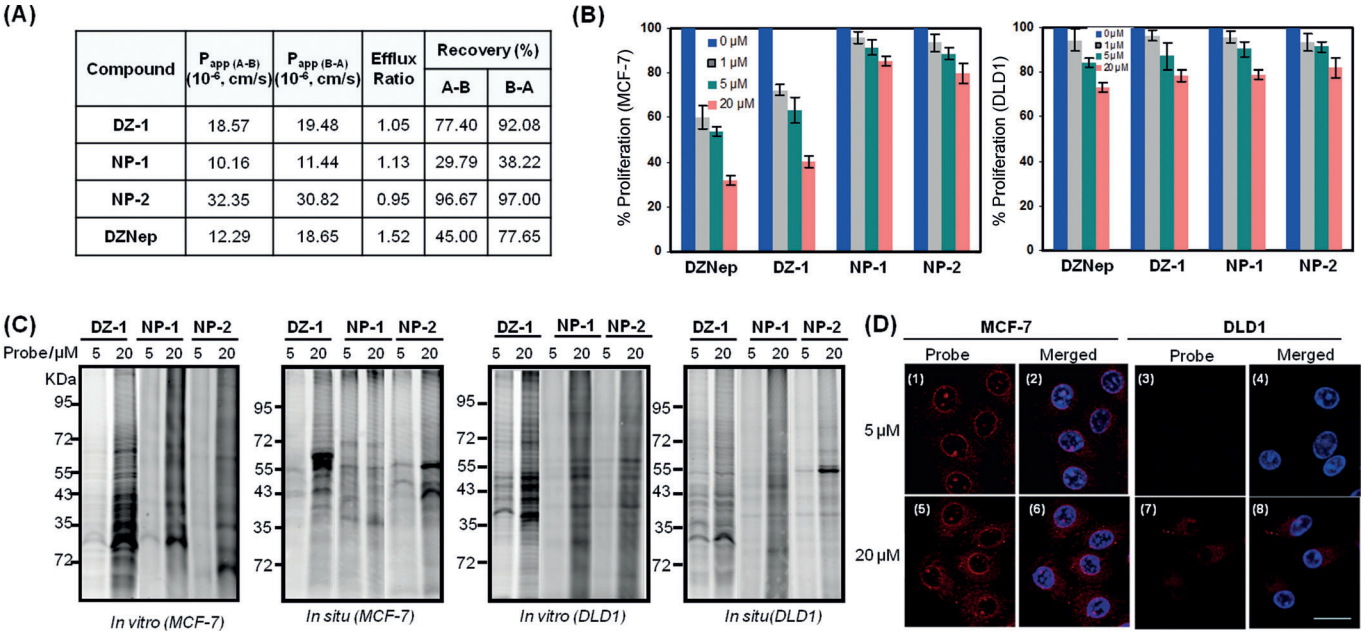

Figure 2. (A) Results of the cell-permeability assay with the three probes and DzNep. (B) Dose-dependent inhibition of cell proliferation in MCF-7 and DLD1 cancer cells with DzNep and the three probes (**DZ-1**, **NP-1**, and **NP-2**) by using the XTT anti-proliferation assay. The data represent the average and standard deviation for two trials. (C) In-vitro and in-situ proteome labeling profiles of MCF-7 and DLD1 by the three probes at different probe concentrations (5 and 20 μM). Only the in-gel fluorescence scanning profiles are shown. (D) Bioimaging of MCF-7 and DLD1 cells treated with **DZ-1** (5 and 20 μM). Panels 1, 3, 5, and 7: Cells treated with the probe followed by click chemistry with rhodamine-N_3; panels 2, 4, 6, and 8: Merged images of the images shown in panels 1, 3, 5, and 7 with Hoechst-stained nuclei (pseudocolored in blue). Scale bar, 10 μm.

cell permeability. To confirm this expectation, we subjected all three probes (**DZ-1**, **NP-1**, and **NP-2**) and DzNep to a bi-directional permeability assay in MDCK cells and the results are summarized in Figure 2A. With apparent permeability (P_{app}) values of 18.57, 10.16, and 32.35 $\mu m\,s^{-1}$ for **DZ-1**, **NP-1**, and **NP-2**, respectively, all three probes had excellent cell permeability that is comparable to that of DzNep, which gave a P_{app} value of 12.29 $\mu m\,s^{-1}$ under identical assay conditions. These results indicate that our DzNep-derived probes are suitable for experiments in live cells.

DzNep is known to induce apoptotic cell death in a number of cancer cells, such as MCF-7 (breast cancer), but not in normal cells.[2a,5] In addition, a combination treatment of DzNep and suberoylanilide hydroxamic acid (SAHA), which is a well-known histone deacetylase inhibitor on DLD-1 cells (a colorectal cancer cell line) was found to effectively induce cell death (unpublished results).[1b,6] In order to determine whether **DZ-1** and DzNep possess similar cellular activities, we performed anti-proliferative assays against MCF-7 and DLD1 cell lines to compare their cell-killing activities (Figure 2B). Following drug treatment for 72 h, both DzNep and **DZ-1** showed good anti-proliferative activities against MCF-7 cells. The effect was dose-dependent and noticeable even at concentrations as low as 1 μM. Side-by-side comparison of the two compounds showed that DzNep consistently displayed a slightly higher cell-killing effect than **DZ-1** at all tested concentrations, thus indicating that the structural modifications introduced into **DZ-1** did cause marginal but tolerable changes in the probe's cellular activities. The fact that neither **DZ-1** nor DzNep showed any effect against DLD1 cells indicates that these compounds alone were insufficient to induce apoptotic cell death in this cell line. The two negative control probes, **NP-1** and **NP-2**, showed no apparent inhibitory activities against either MCF-7 or DLD1 cell growth. This is expected as neither probe possesses the two obligatory structural features of DzNep. Our results thus indicate that **DZ-1** likely preserved most if not all of DzNep's original biological and cellular activities, and therefore may be used for subsequent cell-based proteome profiling experiments for large-scale identification of potential cellular targets (on- and off-targets) of DzNep.

In-Vitro and In-Situ Proteome Profiling

Next, we carried out endogenous proteome labeling, under both in-vitro (cell lysates) and in-situ (live cells) settings, using both MCF-7 and DLD1 cell lines. All three probes (**DZ-1**, **NP-1**, and **NP-2**) were run side-by-side to compare their proteome labeling profiles under two different probe concentrations (5 and 20 μM). Upon probe labeling, followed by rhodamine-N_3 click chemistry, the resulting samples were separated by SDS-PAGE and visualized by in-gel fluorescence scanning (Figure 2C). Relatively weak fluorescence labeling profiles were observed for both negative probes (**NP-1** and **NP-2**) at both low and high concentrations (e.g., 5 and 20 μM, respectively), thus indicating that neither probe had any significant number of specific cellular targets. On

the other hand, **DZ-1** showed weak labeling at 5 μM probe concentration, but at 20 μM probe concentration strongly labeled bands, which likely corresponded to specific cellular targets of the probe, started to appear. This indicates that the effective cellular concentraction of **DZ-1** was relatively high. The overall number and intensity of the fluorescent bands produced by **DZ-1** labeling were consistently higher than those produced by the two negative probes (e.g., **NP-1** and **NP-2**) under the same probe concentrations in both MCF-7 and DLD1 cell lines. This result also indicates that more cellular proteins were targeted by **DZ-1** in identical proteome environments. There were obvious differences in the in-vitro and in-situ proteome profiles of both MCF-7 and DLD1 produced by **DZ-1**, suggesting that the cellular targets of this probe might be different under different cellular settings. Similar results were observed in our previous cell-based proteome profiling studies.[12] This underscores the significance of our approach in its ability to label endogenous protein targets in live cells in their native cellular environments. There were clear differences in the labeling between the two cell lines, under both in-vitro and in-situ settings, indicating that DzNep likely has different cellular targets in MLC-7 and DLD1 cells. Both in-vitro and in-situ proteome profiling experiments were repeated on cells pretreated with an excessive amount of DzNep (Figure S1 in the Supporting Information). The results showed that most **DZ-1** labeled bands were effectively competed away, indicating that these labeled proteins were likely true cellular targets of DzNep.

Bioimaging

There has been enormous interest in the development of small-molecule-based imaging probes capable of reporting in-vivo protein–drug interactions as well as enzymatic activities.[17–19] In some recent examples, several groups have successfully reported small-molecule probes that could be used to image different endogenous kinases in live cells.[12c,19] Given the excellent cell permeability of **DZ-1**, as well as its ability to closely imitate endogenous cellular activities of DzNep, we wondered if this probe could also serve as a useful imaging reagent to study the cellular uptake and localization of DzNep in live mammalian cells. It should be noted that, since DzNep could likely bind to a variety of different cellular proteins, **DZ-1** would therefore not be very useful in bioimaging of specific protein targets. We carried out live-cell imaging experiments in MCF-7 and DLD1 cells using **DZ-1**. First, the cells were treated with **DZ-1** (5 and 20 μM) for 2 h. No cell death was observed at the end of probe treatment. Subsequently, the cells were irradiated by UV light to initiate covalent protein–probe linkage, thereby "fixing" the probe to its cellular targets/locations. Cells were then fixed with formaldehyde, permeabilized by using Triton X-100, and treated with rhodamine-N_3 following our previously optimized click chemistry protocols.[12c] The same cells were further stained with Hoechst to visualize their nuclei. Finally, the cells were imaged by confocal fluorescence microscopy (Figure 2D). In MCF-7 cells, strong fluorescence signals were observed throughout the whole cell excluding the nucleus at 20 μM probe concentration. When the probe concentration was decreased to 5 μM, there was a corresponding decrease in the overall fluorescence signals of the cells, with most of the fluorescence localized mainly on the edge of cell nuclei, indicating that, upon uptake into cells, DzNep likely was localized to these regions under physiological settings. In DLD1 cells, we only observed significant fluorescence signals at 20 μM probe concentration, which was in accordance with both the anti-proliferative results and the in-situ proteome labeling experiments (Figure 2B and 2C) that suggested that DzNep had fewer cellular targets in this cell line. Of the two putative cellular targets of DzNep, SAHH is a cytosolic protein and EZH2 is localized to the nucleus of mammalian cells. The fact that our imaging results showed mostly cytosolic but not nuclear localization of the **DZ-1** probe provides yet another line of evidence that DzNep likely has many other unknown cellular targets that reside outside of the cell nucleus. The endogenous expression of EZH2 was either too low to be detected by the probe, or EZH2 may not be a true cellular target of DzNep (see below).

Large-Scale Pull-Down/LC-MS/MS Analysis

Finally, we performed large-scale pull-down/LC-MS/MS experiments on live MCF-7 cells in situ labeled with **DZ-1**, **NP-1**, and **NP-2** to identify potential cellular targets of DzNep using previously published procedures, with some modifications.[12c] **NP-1** and **NP-2** were used as the negative control probes in order to subtract background protein labeling originating from intrinsic non-specific labeling caused by photo-crosslinking experiments.[14] Protein extracts from the labeled cells were enriched (following click-chemistry conjugation with biotin-N_3) by avidin-agarose beads, separated by SDS-PAGE (see Figure S2 in the Supporting Information), subjected to in-gel trypsin digestion, and identified by LC-MS/MS analysis. The complete LCMS results of all three probes are shown in the Supporting Information, with selected results summarized in Figure 3. As in the case with most large-scale LC-MS/MS experiments, a large number of proteins hits were identified in our results (>1000 different proteins). Among them, many were inevitably highly abundant, nonspecific proteins that were labeled indiscriminately in live cells due to their "sticky" nature and high levels. As a result, they were labeled by all three probes. These proteins were automatically eliminated as false positives. Of the remaining proteins, we focused on those that met the following two criteria: 1) proteins with an exponentially modified protein abundance index (emPAI) value of greater than 0.1, and 2) proteins with a protein score of greater than 30. The emPAI offers an approximate, label-free, relative quantitation of proteins in our pull-down samples based on the protein concentration. In total, there were 41 such proteins present and they were deemed likely true binders of **DZ-1**. When we further grouped these proteins based on their

(A)

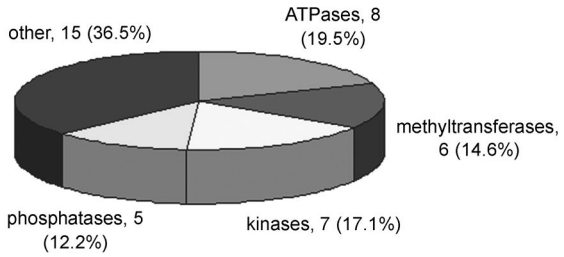

(B)

Protein name	Protein MS	Score	emPAI ratio
Isoform 1 of Histone-arginine methyltransferase	63989	34	∞
S-adenosylmethionine synthase isoform type-2	43975	93	∞
ATPase, Na+/K+ transporting, alpha 2 (+) polypeptide	112046	55	∞
ATP synthase subunit O, mitochondrial	23377	39	∞
Serine/threonine-protein phosphatase	35669	35	∞
Isoform 2 of Protein phosphatase methylesterase 1	22732	34	∞
Sodium/potassium-transporting ATPase subunit beta-3	31834	37	∞
cAMP-dependent protein kinase catalytic subunit alpha	39911	41	∞
Mitogen-activated protein kinase 3	36170	30	∞

Figure 3. (A) The number and percentage of each protein subgroup enriched from the MCF-7 cell line. (B) Representative proteins hits identified from MCF-7 cells. "∞" signals detection only in positive PD/LC-MS/MS (see the Supporting Information for details).

functions (Figure 3A), we found 6 methyltransferases, 7 kinases, 8 ATPases, and 5 phosphatases, most of which possess a nucleotide-binding pocket in their active sites and therefore likely have an intrinsic binding affinity toward DzNep as well. Some of the most interesting proteins hits are also summarized in the table shown in Figure 3B. Both MAPK and PKA, which are well-known protein kinases, as well as histone arginine methyltransferase and phosphatase methyltransferase, which like EZH2 are methyltransferases that utilize *S*-adenosylhomocysteine as a cofactor, are well represented in this list. While our list of potential cellular protein targets of DzNep shown in Figure 3 should be further validated by other independent experiments and more detailed biological studies, the results themselves clearly support the assumption we set out to confirm at the start of the current study, that is, compounds such as DzNep, given their structural homology to adenosine, are likely binders to a variety of cellular proteins. Interestingly, neither SAHH nor EZH2 was positively identified from our LCMS results (see the Supporting Information). This again indicates that either both proteins were not endogenously expressed to a significant extent to be effectively labeled by **DZ-1** in our experiments or that they are not true cellular targets of DzNep.

Conclusions

We have successfully developed a "clickable", cell-permeable probe, **DZ-1**, suitable for cell-based proteome profiling and target identification of DzNep in live MCF-7 cells. The probe possessed similar cell permeability and cellular apoptotic activities as the wild-type DzNep. Through a cell bioimaging experiment we confirmed that **DZ-1** might be useful for the study of cellular uptake and cellular localization of DzNep. From our in-situ large-scale pull-down/LC-MS/MS results, we have successfully obtained a list of potential cellular targets (on- and off-targets) of DzNep. Among the list were several kinases, phosphatases, ATPases, and methyltransferases. Although further studies will be needed in order to validate some of these newly identified, potential DzNep targets, our current findings show that DzNep likely has many unknown cellular targets and that both existing putative targets, EZH2 and SAHH, might not be true targets of DzNep under native cellular settings. Our findings should have important implications in the consideration of using DzNep as a validated chemical probe for epigenetic research (especially against EZH2) and as a potential drug candidate for cancer therapy. Finally, our strategy should be generally useful for the off-target identification of other suitable drugs and/or candidates.

Experimental Section

General Information

All chemicals were purchased from Aldrich or Alfa Aesar and used as received, unless specified otherwise. Dried solvents (CH_2Cl_2, DMF, THF, acetonitrile, Et_2O, and toluene) were drawn from a Glass Contour solvent dispensing system. All reactions requiring anhydrous conditions were carried out under argon atmosphere using oven-dried glassware. The reaction progress was monitored by thin-layer chromatography (TLC) on pre-coated silica plates (Merck 60 F_{254}, 0.25 μm), and spots were visualized by UV light or phosphomolybdic acid stain. Flash column chromatography was carried out using Merck 60 F_{254}, 0.040–0.063 μm silica gel. ^1H and ^{13}C NMR spectra were recorded on a Bruker 400 MHz instrument equipped with a CryoProbe. Chemical shifts for protons are reported in parts per million (ppm) that were referenced to the NMR solvent ($CDCl_3$: 7.26 ppm; $[D_6]$DMSO: 2.50 ppm; CD_3OD: 3.31 ppm). Chemical shifts for carbon are given in ppm that were referenced to the solvent ($CDCl_3$: 77.0 ppm; $[D_6]$DMSO: 39.5 ppm; CD_3OD: 49.0 ppm). Data are presented as follows: chemical shift, multiplicity (br = broad, s = singlet, d = doublet, t = triplet, q = quartet, m = multiplet), integration and coupling constants (*J*) in Hertz (Hz). Electron impact mass spectra (EIMS) (low and high resolution) were measured using a Finnigan MAT95XP double-focusing mass spectrometer. Electrospray ionization (ESI) mass spectra were recorded using a Waters Quattro MicroTM API instrument for low-resolution and an Agilent 6210 Time-of-Flight LC/MS instrument for high-resolution mass spectrometry. In-gel fluorescence scanning of SDS-PAGE gels was carried out with a Typhoon 9410 fluorescence gel scanner (Amersham Biosciences), and where appli-

cable, bands were quantified using ImageQuant 3.3 (Molecular Dynamics). Tris(2-carboxyethyl) phosphine (TCEP) and tris[(1-benzyl-1H-1,2,3-triazol-4-yl)methyl]amine ("ligand") were purchased from Sigma–Aldrich. Hoechst 33342 was purchased from Invitrogen. DzNep (SML0305) was purchased from Sigma–Aldrich. MCF-7 mammalian cells were grown in Dulbecco's modified Eagle's medium (DMEM, Invitrogen, Carlsbad, CA) containing 10% heat-inactivated fetal bovine serum (FBS; Invitrogen), 100 U mL^{-1} penicillin, and 100 mg mL^{-1} streptomycin (Thermo Scientific, Rockford, IL), and maintained in a humidified 37°C incubator with 5% CO_2. Rhodamine-N_3 and biotin-N_3 were synthesized as previously reported.[12]

Synthesis

*6-Chloro-9-((3aS,4R,6aR)-2,2-dimethyl-6-((trityloxy)methyl)-4,6a-dihydro-3aH-cyclopenta[d][1,3]dioxol-4-yl)-9H-purin-2-amine (**2**)*

To a solution of 2-amino-6-chloropurine (751 mg, 4.43 mmol) in anhydrous THF (170 mL) was added **1** (1.46 g, 3.41 mmol, prepared based on previously published procedures[15]) and PPh_3 (1.162 g, 4.43 mmol). Subsequently, diisopropyl azodicarboxylate (DIAD, 872 μL, 4.43 mmol) was added dropwise and the reaction was stirred at 50°C for 18 h under reflux conditions. Following removal of the solvent under reduced pressure, the resulting residue was purified by flash chromatography (Et_2O/petroleum ether, 10:90→60:40) to afford the desired product **2** (1.56 g; 95%) as a white solid. ^{1}H NMR (400 MHz, $CDCl_3$): δ=7.62 (s, 1H), 7.52–7.38 (m, 6H), 7.36–7.20 (m, 9H), 5.97 (brs, 1H), 5.49 (brs, 1H), 5.26 (d, J=5.5 Hz, 1H), 4.66 (d, J=5.5 Hz, 1H), 4.03 (d, J=16.0 Hz, 1H), 3.87 (d, J=16.0 Hz, 1H), 1.43 (s, 3H), 1.33 ppm (s, 3H); ^{13}C NMR (101 MHz, $CDCl_3$): δ=159.0, 153.4, 151.4, 150.4, 143.6, 140.4, 128.5, 128.8, 127.2, 125.7, 121.4, 112.6, 87.3, 84.1, 84.1, 77.3, 64.3, 61.3, 27.5, 26.1 ppm; HR-MS (ESI$^+$) m/z calcd for $C_{33}H_{31}ClN_5O_3$: 580.2115 $[M+H]^+$, found 580.2118.

*6-Chloro-9-((3aS,4R,6aR)-2,2-dimethyl-6-((trityloxy)methyl)-4,6a-dihydro-3aH-cyclopenta[d][1,3]dioxol-4-yl)-2-iodo-9H-purine (**3**)*

To a solution of **2** (1.56 g, 2.69 mmol) in anhydrous acetonitrile (54 mL) was added CuI (51.2 mg, 0.27 mmol) and CH_2I_2 (10.8 mL, 134.5 mmol). The reaction was then cooled to 0°C while *n*-butyl nitrite (1.57 mL, 13.5 mmol)[20] was added. Subsequently, the reaction was heated to 50°C and further stirred for 3 h. Acetonitrile was removed under reduced pressure and the resulting mixture was dissolved in CH_2Cl_2, washed with diluted bicarbonate, dried over Na_2SO_4, filtered, and concentrated in vacuo. Purification by flash chromatography (Et_2O/petroleum ether, 20:80→50:50) afforded the desired product **3** as a pale yellow foam (1.86 g; 80%). ^{1}H NMR (400 MHz, $CDCl_3$): δ=7.87 (s, 1H), 7.48–7.40 (m, 6H), 7.36–7.20 (m, 9H), 5.94 (brs, 1H), 5.64 (brs, 1H), 5.33 (d, J=5.5 Hz, 1H), 4.72 (d, J=5.5 Hz, 1H), 4.05 (d, J=16.0 Hz, 1H), 3.89 (d, J=16.0 Hz, 1H), 1.43 (s, 3H), 1.33 ppm (s, 3H); ^{13}C NMR (101 MHz, $CDCl_3$): δ=152.1, 151.2, 150.6, 143.7, 143.6, 132.1, 128.5, 128., 127.9, 127.3, 121.0, 112.9, 87.4, 84.3, 84.1, 65.2, 61.3, 27.5, 26.2 ppm; HR-MS (ESI$^+$) m/z calcd for $C_{33}H_{30}IN_5O_3$: 671.1393 $[M+H]^+$, found: 671.1399.

*9-((3aS,4R,6aR)-2,2-Dimethyl-6-((trityloxy)methyl)-4,6a-dihydro-3aH-cyclopenta[d][1,3]dioxol-4-yl)-2-iodo-9H-purin-6-amine (**4**)*

To a solution of **3** (1.134 g, 1.64 mol) in THF (16.4 mL) was added 33% NH_3 (8.2 mL) in a sealed tube. The reaction was heated to 50°C and allowed to stir for 6 h. Next, THF was removed under reduced pressure and the mixture was dissolved in CH_2Cl_2, washed with brine, dried over Na_2SO_4, filtered, and concentrated in vacuo to afford pure **4** (1.1 g, 100%) as a white solid. ^{1}H NMR (400 MHz, $CDCl_3$): δ=7.71 (s, 1H), 7.49–7.37 (m, 6H), 7.36–7.20 (m, 9H), 6.30 (s, 2H), 5.93 (d, J=0.9 Hz, 1H), 5.60 (s, 1H), 5.33–5.27 (m, 1H), 4.71 (d, J=5.5 Hz, 1H), 4.03 (d, J=15.5 Hz, 1H), 3.88 (d, J=15.5 Hz, 1H), 1.41 (s, 3H), 1.33 ppm (s, 3H); ^{13}C NMR (101 MHz, $CDCl_3$): δ=154.2, 151.0, 149.6, 146.9, 143.7, 138.4, 128.5, 128.0, 127.9, 127.2, 121.3, 112.8, 87.4, 84.3, 84.2, 65.0, 61.3, 27.5, 26.2 ppm; HR-MS (ESI$^+$) m/z calcd for $C_{33}H_{31}IN_5O_3$: 672.1472 $[M+H]^+$, found 672.1462.

*2-Azido-9-((3aS,4R,6aR)-2,2-dimethyl-6-((trityloxy)methyl)-4,6a-dihydro-3aH-cyclopenta[d][1,3]dioxol-4-yl)-9H-purin-6-amine (**5a**)*

To a solution of CuI (31.2 mg, 0.164 mmol) and *N,N*-dimethylethylene diamine (53 μL, 0.49 mmol) in water (22 mL) was added NaN_3 (213 mg, 3.276 mmol) to form the catalyst mixture. Subsequently, this mixture was added to a microwave vial containing **4** (1.1 g, 1.63 mmol) in EtOH (52 mL). The resulting suspension was heated in a microwave reactor at 90°C for 90 min. Next, EtOH was removed under reduced pressure and the mixture was dissolved in CH_2Cl_2, washed with brine, dried over Na_2SO_4, filtered, and concentrated in vacuo. Further purification by flash chromatography (EtOAc/petroleum 40:60→70:30, followed by MeOH/CH_2Cl_2 3:97→6:94) afforded the azido product **5a** (610 mg; 61%) and the amine side-product **5b** (100 mg, 11%). **5a**: ^{1}H NMR (400 MHz, $CDCl_3$): δ=7.53–7.39 (m, 6H), 7.37–7.21 (m, 9H), 5.97 (brs, 2H), 5.49 (brs, 1H), 5.25 (s, 1H), 5.10 (s, 1H), 4.65 (brs, 1H), 4.10 (d, J=15.5 Hz, 1H), 3.85 (d, J=15.5 Hz, 1H), 1.42 (s, 3H), 1.32 ppm (s, 3H); ^{13}C NMR (101 MHz, $CDCl_3$): δ=156.9, 150.2, 146.9, 143.7, 128.5, 127.9, 127.9, 127.2, 121.5, 112.6, 87.3, 84.5, 84.2, 65.2, 61.5, 27.5, 26.1 ppm; HR-MS (ESI$^+$) m/z calcd for $C_{33}H_{30}N_8O_3$: 287.2589 $[M+H]^+$, found 587.2498. **5b**: ^{1}H NMR (400 MHz, $CDCl_3$): δ=7.46 (dd, J=3.30, 5.31 Hz, 6H), 7.33–7.19 (m, 9H), 5.98 (s, 1H), 4.88 (d, J=5.46 Hz, 1H), 4.74 (t, J=5.44 Hz, 1H), 4.58 (s, 1H), 3.88 (d, J=14.26 Hz, 1H), 3.67 (d, J=14.28 Hz, 1H), 2.71 (d, J=9.18 Hz, 1H), 1.37 ppm (s, 6H); HR-MS (ESI$^+$) m/z calcd for $C_{33}H_{33}N_6O_3$: 561.2614 $[M+H]^+$, found 561.2593.

*2-Azido-9-((3aS,4R,6aR)-2,2-dimethyl-6-((trityloxy)methyl)-4,6a-dihydro-3aH-cyclopenta[d][1,3]dioxol-4-yl)-N,N-diboc-9H-purin-6-amine (**6**)*

To a solution of **5a** (600 mg, 1.02 mmol) in CH_2Cl_2 (51 mL) was added Boc anhydride (893 mg, 4.09 mmol) and DMAP (25 mg, 0.205 mmol). The reaction was allowed to stir at room temperature for 4 h. Following the removal of CH_2Cl_2 under reduced pressure, the resulting residue was purified by flash chromatography (EtOAc/petroleum ether, 10:90→35:65) to afford the desired product **6** (780 mg, 89%) as a white foam. ^{1}H NMR (400 MHz, $CDCl_3$): δ=7.85 (s, 1H), 7.50–7.38 (m, 6H), 7.35–7.18 (m, 9H), 5.97 (s, 1H), 5.59 (s, 1H), 5.36–5.27 (m, 1H), 4.74 (d, J=5.5 Hz, 1H), 4.02 (d, J=15.5 Hz, 1H), 3.87 (d, J=15.5 Hz, 1H), 1.48 (s, 18H), 1.42 (s, 3H), 1.32 ppm (s, 3H); ^{13}C NMR (101 MHz, $CDCl_3$): δ=155.9, 154.3, 151.3, 150.5, 150.3, 143.7, 142.9, 128.5, 127.9, 127.2, 126.2, 121.4, 112.7, 87.4, 84.4, 84.2, 84.1, 65.0, 61.4, 27.8, 27.5, 26.1 ppm.

*((3aR,6R,6aS)-6-(2-Azido-6-(dibocamino)-9H-purin-9-yl)-2,2-dimethyl-6,6a-dihydro-3aH-cyclopenta[d][1,3]dioxol-4-yl)methanol (**7**)*

To a solution of **6** (780 mg, 0.99 mmol) in acetone (9.9 mL) was added 2,2-dimethoxypropane (10.32 mL, 9.91 mmol) and *p*-toluenesulfonic acid dihydrate (95.26 mg, 0.50 mmol). The reaction was allowed to stir at room temperature for 18 h, and stopped by quenching with saturated bicarbonate until the pH of the solution was basic. Following removal of acetone under reduced pressure, the resulting mixture was dissolved in CH_2Cl_2, washed with brine, dried over Na_2SO_4, filtered, and concentrated in vacuo. Further purification by flash chromatography (EtOAc/petroleum ether, 10:90→100:0) afforded the desired product **7** (400 mg, 74%) as a white solid. ^{1}H NMR (400 MHz, $CDCl_3$): δ=7.90 (s, 1H), 5.73 (s, 1H), 5.54 (s, 1H), 5.47 (d, J=5.5 Hz, 1H), 4.78 (d, J=5.5 Hz, 1H), 4.52–4.39 (m, 2H), 1.52–1.44 (m, 21H), 1.37 ppm (s, 3H); ^{13}C NMR (101 MHz, $CDCl_3$): δ=156.3, 154.0, 152.3, 150.9, 150.0, 143.0, 124.0, 121.5, 113.0, 84.6, 84.3, 84.2, 65.3, 59.9, 27.9, 27.8, 27.4, 25.9 ppm; HR-MS (ESI$^+$) m/z calcd for $C_{24}H_{33}N_8O_7$: 545.2472$[M+H]^+$, found 545.2469.

*(3aR,6R,6aS)-6-(2-Azido-6-(dibocamino)-9H-purin-9-yl)-2,2-dimethyl-6,6a-dihydro-3aH-cyclopenta[d][1,3]dioxole-4-carbaldehyde (**8**)*

To a solution of **7** (186 mg, 0.34 mmol) in CH_2Cl_2 (3.4 mL) was added Dess–Martin periodinane (DMP, 174 mg, 0.41 mmol), and the reaction was allowed to stir at room temperature for 2 h. Next, the reaction mixture was filtered through a pack of Celite (2 times). Upon removal of CH_2Cl_2 in vacuo, the desired product **8** was obtained, which was used directly in the next step without further purification. ^{1}H NMR (400 MHz, $CDCl_3$): δ=9.96 (s, 1H), 7.90 (s, 1H), 6.70 (s, 1H), 5.77 (d, J=5.5 Hz,

1H), 5.71 (s, 1H), 4.94 (d, J=5.5 Hz, 1H), 1.49–1.48 (bs, 21H), 1.39 ppm (s, 3H).

*((3aR,6R,6aS)-6-(2-azido-6-(dibocamino)-9H-purin-9-yl)-2,2-dimethyl-6,6a-dihydro-3aH-cyclopenta[d][1,3]dioxol-4-yl)(4-((trimethylsilyl)ethynyl)phenyl)methanol (**9**)*

To a 2-neck round-bottom flask under argon was added magnesium (48.7 mg, 2.0 mmol) in anhydrous THF (1 mL), and the reaction was allowed to stir at 50 °C. Subsequently, a solution of [(4-bromophenyl)ethynyl]trimethylsilane (507 mg, 2.0 mmol) in anhydrous THF (3 mL) was added dropwise to the above mixture, and the reaction was stirred at 50 °C for 30 min under reflux conditions. Next, a small amount of iodine was added to magnesium (9.7 mg, 0.4 mmol) in a separate vial and this was then added to the reaction mixture. Stirring was continued at 50 °C for another 3 h to finally afford 4-[(trimethylsilyl)ethynyl]phenyl magnesium bromide ("the Grignard reagent") as a 0.5 M solution in THF. Subsequently, the above Grignard reagent in THF (2.05 mL, 1.02 mmol) was added to a solution of **8** (185 mg; 0.34 mmol) in anhydrous THF (3.4 mL) under argon, and the reaction was allowed to stir at room temperature for 18 h. The reaction was then quenched with saturated NH_4Cl. Upon removal of THF under reduced pressure, the resulting mixture was dissolved in CH_2Cl_2, washed with brine, dried over Na_2SO_4, filtered, and concentrated in vacuo. Further purification by flash chromatography (EtOAc/petroleum ether, 0:100→50:50) afforded the desired product **9** (139 mg; 56%) as a yellow solid (mixture of isomers 10:1). ^{1}H NMR (400 MHz, $CDCl_3$): δ=7.84 (s, 1H), 7.50 (d, J=8.3 Hz, 2H), 7.38 (d, J=8.3 Hz, 2H), 6.23 (s, 1H), 5.90 (s, 1H), 5.53 (s, 1H), 5.06 (d, J=5.5 Hz, 1H), 4.73 (d, J=5.5 Hz, 1H), 1.57 (s, 9H), 1.49 (s, 3H), 1.44 (s, 9H), 1.31 (s, 3H), 0.26 ppm (s, 9H); ^{13}C NMR (101 MHz, $CDCl_3$): δ=152.3, 152.1, 150.5, 150.3, 149.5, 140.2, 136.4, 132.5, 127.8, 124.1, 121.9, 118.2, 113.2, 104.5, 95.4, 84.2, 83.8, 83.0, 82.9, 75.6, 65.3, 28.2, 27.8, 27.8, 27.4, 26.1, 0.0 ppm; HR-MS (ESI$^+$) m/z calcd for $C_{35}H_{45}N_8O_7Si$: 717.3180 $[M+H]^+$, found 717.3198.

*((3aR,6R,6aS)-6-(2-azido-6-(dibocamino)-9H-purin-9-yl)-2,2-dimethyl-6,6a-dihydro-3aH-cyclopenta[d][1,3]dioxol-4-yl)(4-ethynylphenyl)methanol (**10**)*

To a solution of **9** (139 mg; 0.19 mmol) in anhydrous THF (9.7 mL) was added 1 M tetra-*n*-butylammonium fluoride (TBAF) in THF (233 μL, 0.23 mmol), and the reaction was allowed to stir at room temperature for 2 h, before being quenched with saturated NH_4Cl. Following removal of THF under reduced pressure, the resulting mixture was dissolved in CH_2Cl_2, washed with brine, dried over Na_2SO_4, filtered, and concentrated in vacuo. Further purification by flash chromatography (EtOAc/petroleum ether, 10:90→40:60) afforded **10** (86 mg; 69%) as a yellow solid. ^{1}H NMR (400 MHz, $CDCl_3$): δ=7.72 (s, 1H), 7.54 (d, J=8.1 Hz, 2H), 7.42 (d, J=8.1 Hz, 2H), 6.25 (s, 1H), 5.90 (s, 1H), 5.50 (s, 1H), 5.07 (d, J=5.4 Hz, 1H), 4.74 (d, J=5.4 Hz, 1H), 3.11 (s, 1H), 1.56 (s, 9H), 1.50 (s, 3H), 1.44 (s, 9H), 1.31 ppm (s, 3H); ^{13}C NMR (101 MHz, $CDCl_3$): δ=156.8, 152.2, 150.6, 149.8, 149.5, 140.6, 136.8, 132.7, 127.9, 123.0, 122.2, 119.2, 113.1, 84.1, 83.8, 83.1, 83.0, 82.7, 78.0, 77.2, 75.5, 65.1, 28.1, 27.7, 27.7, 27.4, 26.1 ppm; HR-MS (ESI$^+$) m/z calcd for $C_{32}H_{37}N_8O_7$: 645.2785 $[M+H]^+$, found 645.2772.

*(1S,2R,5R)-5-(6-Amino-2-azido-9H-purin-9-yl)-3-((4-ethynylphenyl)(hydroxy)methyl)cyclopent-3-ene-1,2-diol hydrochloride (**DZ-1**)*

Compound **10** (30 mg, 0.047 mmol) in MeOH (1 mL) was stirred in 2 N HCl (116.7 μL, 0.233 mmol) at room temperature for 18 h. Upon solvent removal under reduced pressure, a yellowish solid was obtained. Purification using reverse-phase preparative HPLC was performed to afford **DZ-1** (17.2 mg, 84%) as a pure white solid. ^{1}H NMR (400 MHz, MeOD): δ=7.94 (s, 1H), 7.54–7.45 (m, 4H), 6.06 (s, 1H), 5.42 (brs, 1H), 5.39 (brs, 1H), 4.36 (apparent, J=5.5 Hz, 1H), 4.26 (d, J=5.5 Hz, 1H), 3.47 ppm (s, 1H); ^{13}C NMR (101 MHz, MeOD): δ=155.9, 154.0, 153.9, 151.2, 143.3, 142.0, 133.3, 128.8, 124.4, 123.5, 114.1, 84.2, 78.9, 78.0, 74.3, 72.6, 68.2 ppm; HR-MS (ESI$^+$) m/z calcd for $C_{19}H_{17}N_8O_3$: 405.1424 $[M+H]^+$, found 405.1345; calcd for $C_{13}H_{16}N_8NaO_3$: 427.1243 $[M+Na]^+$, found 427.1249.

*4-Azidophenyl)methanol (**11**)[21]*

To a stirred solution of (4-aminophenyl)methanol (600 mg, 4.87 mmol) in acetic acid (36 mL) and water (4 mL) was added $NaNO_2$ (672 mg, 9.74 mmol) and then NaN_3 (633 mg, 9.74 mmol) at 0 °C. The reaction mixture was stirred for 30 min and subsequently poured into water and neutralized to pH 7 by slow addition of solid $NaHCO_3$. The resulting mixture was extracted with EtOAc. The combined layer was washed with water and brine, dried over Na_2SO_4, filtered, and concentrated in vacuo. The residue was purified by flash chromatography (EtOAc/petroleum ether, 0:100→15:85) to afford **11** (600 mg, 83%) as a colorless oil. ^{1}H NMR (400 MHz, $CDCl_3$): δ=7.35 (d, J=8.6 Hz, 2H), 7.02 (d, J=8.5 Hz, 2H), 4.66 ppm (s, 2H).

*Azido-4-(bromomethyl)benzene (**12**)[21]*

To a solution of **11** (200 mg, 1.34 mmol) in dry CH_2Cl_2 (5 mL) under argon was added CBr_4 (889 mg, 2.68 mmol) and PPh_3 (703 mg, 2.68 mmol) at 0 °C, and the reaction was stirred for 30 min. Following solvent evaporation in vacuo, the resulting residue was purified by flash chromatography (EtOAc/petroleum ether, 0:100→2:98) to afford **12** (218 mg, 77%) as a colorless oil. ^{1}H NMR (400 MHz, $CDCl_3$): δ=7.38 (d, J=8.5 Hz, 2H), 7.00 (d, J=8.5 Hz, 2H), 4.48 ppm (s, 2H).

*1-Azido-4-((pent-4-yn-1-yloxy)methyl)benzene (**NP-1**)*

To a solution of pent-4-yn-1-ol (63 mg, 0.75 mmol) in dry THF (2 mL) was added sodium hydride (23 mg, 0.56 mmol, 60%) under argon at 0 °C. Following stirring for 30 min, a solution of **12** (80 mg, 0.38 mmol) in THF was cannulated, followed by addition of Bu_4NI (70 mg, 0.19 mmol). The reaction mixture was stirred further for 5 h, before being quenched by slow addition of a saturated aqueous NH_4Cl solution. The resulting mixture was then extracted with EtOAc. The combined layer was washed with water and brine, dried over Na_2SO_4, filtered, and concentrated in vacuo. The residue was purified by flash chromatography (EtOAc/petroleum ether, 0:100→5:95) to afford **NP-1** (30 mg, 37%) as a colorless oil. ^{1}H NMR (400 MHz, $CDCl_3$): δ=7.32 (d, J=8.6 Hz, 2H), 7.01 (d, J=8.5 Hz, 2H), 4.48 (s, 2H), 3.57 (t, J=6.2 Hz, 2H), 2.32 (td, J=7.1, 2.7 Hz, 2H), 1.94 (t, J=2.7 Hz, 1H), 1.88–1.77 ppm (m, 2H); ^{13}C NMR (101 MHz, $CDCl_3$): δ=139.3, 135.3, 129.1 (2C), 118.9 (2C), 83.8, 72.4, 68.7, 68.5, 28.6, 15.3 ppm; FTIR (neat): $\tilde{\nu}_{max}$=3302, 2256, 2110, 1507 cm^{-1}; HR-MS (ESI$^+$) m/z calcd for $C_{12}H_{13}N_3NaO$: 238.0951 $[M+Na]^+$, found 238.0961.

*6-Chloro-9-(pent-4-yn-1-yl)-9H-purin-2-amine (**13**)*

To a suspension of 2-amino-6-chloropurine (1.5 g, 8.85 mmol) in anhydrous THF (30 mL) under argon was sequentially added pent-4-yn-1-ol (1.63 mL, 17.69 mmol), PPh_3 (5.8 g, 22.12 mmol), and DIAD (4.36 mL, 22.12 mmol). The reaction mixture was stirred at 50 °C for 18 h under reflux conditions. Following evaporation of THF under reduced pressure, the residue was purified by flash chromatography (MeOH/$CHCl_3$, 1:99→5:95) to afford **13** (500 mg, 24%) as a white solid. ^{1}H NMR (400 MHz, $CDCl_3$): δ=7.79 (s, 1H), 5.10 (s, 2H), 4.24 (t, J=6.8 Hz, 2H), 2.22 (dd, J=6.8, 2.6 Hz, 1H), 2.13–2.01 ppm (m, 4H); ^{13}C NMR (101 MHz, $CDCl_3$): δ=159.0, 153.8, 151.3, 142.5, 125.3, 81.9, 70.3, 42.5, 27.6, 15.6 ppm; HR-MS (ESI$^+$) m/z calcd for $C_{10}H_{11}ClN_5$: 236.0697 $[M+H]^+$, found 236.0700.

*2-Azido-6-chloro-9-(pent-4-yn-1-yl)-9H-purine (**14**)*

To a stirred solution of **17** (156 mg, 0.67 mmol) in dry acetonitrile (4 mL) under argon was added butyl nitrate (780 μL, 6.68 mmol) and TMS-N_3 (877 μL, 6.88 mol) at −15 °C. After stirring at the same temperature for 12 h, the solvent was removed under reduced pressure. The resulting residue was purified by flash chromatography (EtOAc/petroleum ether, 0:100→30:70) to afford **14** (80 mg, 46%) as a white solid. ^{1}H NMR (400 MHz, $CDCl_3$): δ=8.05 (s, 1H), 4.38 (t, J=6.8 Hz, 2H), 2.25 (m, 2H), 2.18–2.08 (m, 2H), 2.06 ppm (t, J=2.6 Hz, 1H); ^{13}C NMR (101 MHz, $CDCl_3$): δ=156.1, 153.3, 152.0, 145.1, 128.9, 81.5, 70.5, 43.0,

27.6, 15.5 ppm; HR-MS (ESI$^+$) m/z calcd for $C_{10}H_9ClN_7$: 262.0602 $[M+H]^+$, found 262.0600.

*2-Azido-9-(pent-4-yn-1-yl)-9 H-purin-6-amine (**NP-2**)*

Compound **14** (25 mg, 0.09 mmol) was heated with methanolic ammonia (3 mL) in a sealed tube at 50 °C for 12 h. The reaction mixture was poured into water and the resulting solid was filtered, washed with water, and dried to afford **NP-2** (9 mg, 39 %) as a white solid. ^{1}H NMR (400 MHz, $CDCl_3$): $\delta = 7.73$ (s, 1 H), 4.24 (t, $J = 6.7$ Hz, 2 H), 2.71 (s, 2 H), 2.17 (td, $J = 6.7$, 2.5 Hz, 2 H), 2.10–1.98 ppm (m, 3 H); ^{13}C NMR (101 MHz, $CDCl_3$): $\delta = 156.8$, 155.9, 151.1, 140.1, 116.3, 81.9, 70.1, 42.5, 27.8, 15.4 ppm; HR-MS (ESI$^+$) m/z calcd for $C_{10}H_{10}N_8Na$: 265.0921 $[M+Na]^+$, found 265.0928.

Cell-Permeability and Proliferation Assays

The cell-permeability assay was carried out, as previously described,[22] with MDCK (Madin–Darby canine kidney) cells and with caffeine and Lucifer yellow as controls. Cell viability was determined using the XTT colorimetric cell-proliferation kit (Roche). Briefly, cells were grown to 20–30 % confluence (as they will reach approximately 90 % confluence within 48 to 72 h in the absence of drugs) in 96-well plates under the conditions described above. The medium was aspirated, washed with PBS, and then treated, in duplicate, with 0.1 mL of the medium containing different concentrations of the probe (1–20 μM) or DzNep (1–20 μM; as a positive control). Probes were applied from DMSO stocks whereby DMSO does not exceed 1 % in the final solution. The same volume of DMSO was used as a negative control. Fresh medium, along with the probes and DzNep, were added every 24 h. After a total treatment time of 72 h, proliferation was assayed using the XTT kit by following the guidelines provided by the manufacturer (read at 450 nm). Data represent the average (±s.d.) of two trials.

In-Vitro and In-Situ Proteome Profiling

For in-vitro labeling, the probe was added to 50 μg of freshly prepared cell lysates (prepared as previously described[12]) in 50 μL of Hepes buffer at a desired concentration. Unless indicated otherwise, samples were incubated for 30 min at room temperature and then irradiated with UV light (254 nm) for 5 min. Four microliters of a freshly premixed click chemistry reaction cocktail in PBS containing 100 μM rhodamine-N_3 (from a 1 mM stock solution in DMSO), 0.1 mM TBTA (from a 2.4 mM freshly prepared stock solution in deionized water), 1 mM TCEP (from a 24 mM freshly prepared stock solution in deionized water), and 1 mM CuSO4 (from a 24 mM freshly prepared stock solution in deionized water) were added. The reaction was further incubated for 2 h with gentle mixing, before it was terminated by the addition of prechilled acetone (0.5 mL; 30 min incubation at −20 °C). Precipitated proteins were subsequently collected by centrifugation (13000 *g* for 10 min at 4 °C). The supernatant was discarded and the pellet was washed with 200 μL of prechilled MeOH. Subsequently, the sample was heated at 95 °C in 2× SDS loading buffer for 10 min. Around 20 μg (per gel lane) of proteins were separated by SDS-PAGE (10 % gel) and then visualized by in-gel fluorescence scanning. For in-situ labeling, cells were grown to 80–90 % confluence in 6-well plates under conditions described above. The medium was removed, and cells were washed twice with cold PBS and then treated with 0.5 mL of probe-containing DMEM (the probe was diluted from DMSO stocks whereby DMSO never exceeded 1 % in the final solution). After 5 h of incubation at 37 °C under 5 % CO_2, the medium was aspirated, and cells were washed gently with PBS (2×) to remove excess probe, followed by UV irradiation for 5 min on ice. The cells were then trypsinized and pelleted by centrifugation. Subsequently, the cell pellets were resuspended in PBS (50 μL), homogenized by sonication, and diluted to 1 mg mL^{-1} with PBS. All subsequent procedures were similar to those from in-vitro experiments. The protein pellets were then resuspended in 20 μL of 1× SDS loading buffer and heated for 10 min at 95 °C. Around 20 μg (per gel lane) of proteins were separated by SDS-PAGE (10 % gel) and then visualized by in-gel fluorescence scanning.

Cellular Imaging in MCF-7 Cells

MCF-7 cells were seeded in glass bottom dishes (Mattek) and grown until 70–80 % confluence.[12c] Cells were then treated with 0.5 mL of DMEM containing the probe at different concentrations. After 2 h at 37 °C, the medium was removed, and cells were gently washed twice with PBS, followed by UV irradiation (254 nm) for 5 min. The cells were subsequently fixed for 15 min at room temperature with 3.7 % formaldehyde in PBS, washed twice with cold PBS, and permeabilized with 0.1 % Triton X-100 in PBS for 10 min. Cells were then blocked with 2 % BSA in PBS for 30 min, washed twice with PBS, and subsequently treated with a freshly prepared premixed click chemistry reaction solution in a volume of 100 μL (final concentrations of reagents: 1 mM $CuSO_4$, 1 mM TCEP, 100 μM TBTA, and 10 μM rhodamine-N_3 in PBS) for 2 h at room temperature under vigorous shaking. Cells were washed with PBS at least three times. The same cells were then incubated in PBS containing 0.25 mg mL^{-1} of Hoechst for 15 min at room temperature to stain nuclear DNA, and washed with PBS for 5 min with gentle agitation and a final wash with deionized water (1–2 min with gentle agitation) before mounting. Cellular imaging was done using a Leica TCS SP5X confocal microscope system equipped with Leica HCX PL APO 63×/1.20 W CORR CS, 405 nm diode laser, white laser (470–670 nm, with 1 nm increments, with eight channels AOTF for simultaneous control of eight laser lines, each excitation wavelength provides 1.5 mV), and a photomultiplier tube (PMT) detector ranging from 410 to 700 nm for steady-state fluorescence. Images were processed with Leica Application Suite Advanced Fluorescence (LAS AF).

Pull-Down (PD) and LC-MS/MS Analysis

The general in-situ proteome labeling and pull-down procedures were based on previously reported procedures,[12] with the following optimizations. Briefly, the probe (10 μM) was directly added to live MCF-7 cells, followed by incubation for 5 h at 37 °C under 5 % CO_2. DMSO never exceeded 1 % in the final solution. The medium was aspirated, and cells were washed twice gently with PBS to remove excess probe, followed by UV irradiation (254 nm) for 5 min on ice. The cells were then trypsinized and pelleted by centrifugation. Subsequently, the cell pellets were resuspended in PBS (50 μL), homogenized by sonication, and diluted to 1 mg mL^{-1} with PBS. The labeled lysates were then subjected to click reaction with biotin-N_3, and all subsequent experiments were carried out as previously described.[12c] Control labeling/PD experiments using the negative probe (**NP-1** or **NP-2** at 10 μM final concentration) was carried out concurrently. After PD, all protein samples were separated on 10 % SDS-PAGE gels, followed by coomassie or silver staining. Trypsin digestion was performed as previously described.[12] Digested peptides were extracted from the gel with 50 % acetonitrile and 1 % formic acid. The peptides were separated and analyzed on a Shimadzu UFLC system (Shimadzu, Japan): A mobile phase A (0.1 % formic acid in H_2O) and mobile phase B (0.1 % formic acid in acetonitrile) were used to establish a 60 min gradient comprising 45 min of 5–35 % B, 8 min of 35–50 % B, and 2 min of 80 % B, followed by re-equilibrating at 5 % B for 5 min. Peptides were then analyzed on LTQ-FT mass spectrometer with an Advance CaptiveSpray Source (Michrom Bio Resources) at an electrospray potential of 1.5 kV. A gas flow of 2 L min^{-1}, ion transfer tube temperature of 180 °C, and collision gas pressure of 0.85 mTorr were used. The LTQ-FT was set to perform data acquisition in the positive-ion mode as previously described,[23] except that the m/z range of 350–1600 was used in the full MS scan. The raw data were converted to mgf format. The database search was performed with an in-house Mascot server (version 2.2.07, Matrix Science) with MS tolerance of 10 ppm and MS/MS tolerance of 0.8 Da. Two missed cleavage sites of trypsin were allowed. Carbamidomethylation (C) was set as a fixed modification, and oxidation (M) and phosphorylation (S, T, and Y) were set as variable modifications. LC-MS/MS results obtained from the above experiments (in situ, and for negative probes) were processed as shown below, and results are summarized in the Supporting Information. As in the case of most large-scale LCMS experiments,[12] a large number of proteins were identified from each LCMS run, many of which were "sticky" and/or highly abundant proteins. These were automatically removed. "False" hits that appeared

in negative control pull-down/LCMS experiments were further eliminated. Detailed LC-MS/MS results are presented in the Supporting Information.

Acknowledgements

Funding was provided by the National Medical Research Council (NMRC/1260/2010) and the Agency for Science Technology and Research (A*STAR). The authors thank Mr. Tan Tiong Wei for his help in the scale-up of some compounds and Dr. Yu Qiang for the supply of DLD1 cells. We thank Dr. Siu Kwan Sze (Nanyang Technological University, Singapore) for advice and support concerning LCMS experiments.

[1] a) C. K. Tseng, *J. Med. Chem.* **1989**, *32*, 1442–1446; b) C. L. L. Chai, E. K. W. Tam, H. Y. Yang, T. M. Nguyen, Q. Yu, WO2010036213A1.
[2] a) J. Tan, X. Yang, L. Zhuang, X. Jiang, W. Chen, P. L. Lee, R. K. M. Karuturi, P. B. O. Tan, E. T. Liu, Q. Yu, *Genes Dev.* **2007**, *21*, 1050–1063; b) A. Chase, N. C. P. Cross, *Clin. Cancer Res.* **2011**, *17*, 2613–2618; c) J. A. Simon, C. A. Lange, *Mutat. Res.* **2008**, *647*, 21–29.
[3] R. Cao, L. Wang, H. Wang, L. Xia, H. Erdjument-Bromage, P. Tempst, R. S. Jones, Y. Zhang, *Science* **2002**, *298*, 1039–1043.
[4] C. Cardoso, S. Timsit, L. Villard, M. Khrestchatisky, M. Fontes, L. Colleaux, *Hum. Mol. Genet.* **1998**, *7*, 679–684.
[5] a) T. Chiba, E. Suzuki, M. Negishi, A. Saraya, S. Miyagi, T. Konuma, S. Tanaka, M. Tada, F. Kanai, F. Imazeki, A. Iwama, O. Yokosuka, *Int. J. Cancer* **2012**, *130*, 2557–2567; b) C. D. Kemp, M. Rao, S. Xi, S. Inchauste, H. Mani, P. Fetsch, A. Filie, M. Zhang, J. A. Hong, R. L. Walker, Y. J. Zhu, R. T. Ripley, A. Mathur, F. Liu, M. Yang, P. A. Meltzer, V. E. Marquez, A. De Rienzo, R. Bueno, D. S. Schrump, *Clin. Cancer Res.* **2012**, *18*, 77–90; c) Y. D. Benoit, K. B. Laursen, M. S. Witherspoon, S. M. Lipkin, L. J. Gudas, *J. Cell. Physiol.* **2013**, *228*, 764–772.
[6] W. Fiskus, Y. Wang, A. Sreekumar, K. Buckley, H. Shi, A. Juillella, C. Ustun, R. Rao, P. Fernandez, J. Chen, R. Balusu, S. Koul, P. Atadja, V. E. Marquez, K. N. Bhalla, *Blood* **2009**, *114*, 2733–2743.
[7] E. M. Bissinger, R. Heinke, W. Sippl, M. Jung, *MedChemComm* **2010**, *1*, 114–124.
[8] F. Crea, E. Paolicchi, V. E. Marquez, R. Danesi, *Crit. Rev. Oncol. Hematol.* **2012**, *83*, 184–193.
[9] a) U. Rix, G. Superti-Furga, *Nat. Chem. Biol.* **2009**, *5*, 616–624 and references therein; b) M. W. Karaman, S. Herrgard, D. K. Treiber, P. Gallant, C. E. Atteridge, B. T. Campbell, K. W. Chan, P. Cicer, M. I. Davis, P. T. Edeen, R. Faraoni, M. Floyd, J. P. Hunt, D. J. Jockhart, Z. V. Milanov, M. J. Morrison, G. Pallares, H. K. Patel, S. Pritchard, L. M. Wodicka, P. P. Zarrinkar, *Nat. Biotechnol.* **2008**, *26*, 127–132; c) J. J. Fischer, O. Y. Graebner, C. Dalhoff, S. Michaelis, A. K. Schrey, J. Ungewiss, K. Andrich, D. Jeske, F. Kroll, M. Glinski, M. Sefkow, M. Dreger, H. Koester, *J. Proteome Res.* **2010**, *9*, 806–817.
[10] a) M. Bantscheff, D. Eberhard, Y. Abraham, S. Bastuck, M. Boesche, S. Hobson, T. Mathieson, J. Perrin, M. Raida, C. Rau, V. Reader, G. Sweetman, A. Bauer, T. Bouwmeester, C. Hopf, U. Kruse, G. Neubauer, N. Ramsden, J. Rick, B. Kuster, G. Drewes, *Nat. Biotechnol.* **2007**, *25*, 1035–1044; b) J. Du, P. Bernasconi, K. R. Clauser, D. R. Mani, S. P. Finn, R. Beroukhim, M. Burns, B. Julian, X. P. Peng, H. Hieronymus, R. L. Maglathlin, T. A. Lewis, L. M Liau, P. Nghiemphu, I. K. Mellinghoff, D. N. Louis, M. Loda, S. A Carr, A. L. Kung, T. R. Golub et al., *Nat. Biotechnol.* **2009**, *27*, 77–83.
[11] M. Uttamchandani, C. H. S. Lu, S. Q. Yao, *Acc. Chem. Res.* **2009**, *42*, 1183–1192.
[12] a) P.-Y. Yang, K. Liu, M. H. Ngai, M. J. Lear, M. Wenk, S. Q. Yao, *J. Am. Chem. Soc.* **2010**, *132*, 656–666; b) H. Shi, X. Cheng, S. K. Sze, S. Q. Yao, *Chem. Commun.* **2011**, *47*, 11306–11308; c) H. Shi, C.-J. Zhang, G. Y. J. Chen, S. Q. Yao, *J. Am. Chem. Soc.* **2012**, *134*, 3001–3014; d) P.-Y. Yang, M. Wang, C. Y. He, S. Q. Yao, *Chem. Commun.* **2012**, *48*, 835–837.
[13] a) H. C. Kolb, K. B. Sharpless, *Drug Discovery Today* **2003**, *8*, 1128–1137; b) M. Meldal, C. W. Tornøe, *Chem. Rev.* **2008**, *108*, 2952–3015; c) E. M. Sletten, C. R. Bertozzi, *Angew. Chem.* **2009**, *121*, 7108–7133; *Angew. Chem. Int. Ed.* **2009**, *48*, 6974–6998; d) K. A. Kalesh, H. Shi, J. Ge, S. Q. Yao, *Org. Biomol. Chem.* **2010**, *8*, 1749–1762.
[14] a) F. Kotzyba-Hibert, I. Kapfer, M. Goeldner, *Angew. Chem.* **1995**, *107*, 1391–1408; *Angew. Chem. Int. Ed. Engl.* **1995**, *34*, 1296–1312; b) B. J. Leslie, P. J. Hergenrother, *Chem. Soc. Rev.* **2008**, *37*, 1347–1360; c) J. Das, *Chem. Rev.* **2011**, *111*, 4405–4417; d) L. Dubinsky, B. P. Krom, M. M. Meijler, *Bioorg. Med. Chem.* **2012**, *20*, 554–570; e) M. Ueda, Y. Manabe, Y. Otsuka, N. Kanzawa, *Chem. Asian J.* **2011**, *6*, 3286–3297; f) J. Park, S. Oh, S. B. Park, *Angew. Chem.* **2012**, *124*, 5543–5547; *Angew. Chem. Int. Ed.* **2012**, *51*, 5447–5451; g) K. Sakurai, M. Tawa, A. Okada, R. Yamada, N. Sato, M. Inahara, M. Inoue, *Chem. Asian J.* **2012**, *7*, 1567–1571.
[15] J. H. Cho, D. L. Bernard, R. W. Sidwell, E. R. Kern, C. K. Chu, *J. Med. Chem.* **2006**, *49*, 1140–1148.
[16] a) E. W. Chan, S. Chattopadhaya, R. C. Panicker, X. Huang, S. Q. Yao, *J. Am. Chem. Soc.* **2004**, *126*, 14435–14446; b) K. Liu, H. Shi, H. Xiao, A. G. L. Chong, X. Bi, Y. T. Chang, K. Tan, R. Y. Yada, S. Q. Yao, *Angew. Chem.* **2009**, *121*, 8443–8447; *Angew. Chem. Int. Ed.* **2009**, *48*, 8293–8297.
[17] a) V. Biju, T. Itoh, M. Ishikawa, *Chem. Soc. Rev.* **2010**, *39*, 3031–3056; b) T. Terai, T. Nagano, *Curr. Opin. Chem. Biol.* **2008**, *12*, 515–521; c) D. W. Domaille, E. L. Que, C. J. Chang, *Nat. Chem. Biol.* **2008**, *4*, 168–175; d) A. Baruch, D. A. Jeffery, M. Bogyo, *Trends Cell Biol.* **2004**, *14*, 29–35.
[18] a) J. Li, S. Q. Yao, *Org. Lett.* **2009**, *11*, 405–408; b) M. Hu, L. Li, H. Wu, Y. Su, P.-Y. Yang, M. Uttamchandani, Q.-H. Xu, S. Q. Yao, *J. Am. Chem. Soc.* **2011**, *133*, 12009–12020; c) L. Li, J. Ge, H. Wu, Q.-H. Xu, S. Q. Yao, *J. Am. Chem. Soc.* **2012**, *134*, 12157–12167; d) L. Li, X. Shen, Q.-H. Xu, S. Q. Yao, *Angew. Chem.* **2013**, *125*, 442–446; *Angew. Chem. Int. Ed.* **2013**, *52*, 424–428.
[19] a) G. Budin, K. S. Yang, T. Reiner, R. Weissleder, *Angew. Chem.* **2011**, *123*, 9550–9553; *Angew. Chem. Int. Ed.* **2011**, *50*, 9378–9381; b) K. S. Yang, G. Budin, T. Reiner, C. Vinegoni, R. Weissleder, *Angew. Chem.* **2012**, *124*, 6702–6707; *Angew. Chem. Int. Ed.* **2012**, *51*, 6598–6603.
[20] I. A. Dubery, A. E. Louw, F. R. van Heerden, *Photochemistry* **1999**, *50*, 983–989.
[21] M. Belkheira, D. El Abed, J.-M. Pons, C. Bressy, *Chem. Eur. J.* **2011**, *17*, 12917–12921.
[22] H. Wu, J. Ge, S. Q. Yao, *Angew. Chem.* **2010**, *122*, 6678–6682; *Angew. Chem. Int. Ed.* **2010**, *49*, 6528–6532.
[23] C. S. Gan, T. Guo, H. Zhang, S. K. Kim, S. K. Sze, *J. Proteome Res.* **2008**, *7*, 4869–4877.

Received: March 7, 2013
Revised: April 11, 2013
Published online: June 7, 2013

